Rev. Roum. Sci. Techn.– Électrotechn. et Énerg.
Vol. **67**, *2*, pp. 93–98, Bucarest, 2022

Électrotechnique et électroénergétique

THREE-LEVEL DIRECT TORQUE CONTROL BASED ON BALANCING STRATEGY OF FIVE-PHASE INDUCTION MACHINE

ELAKHDAR BENYOUSSEF[1], SAID BARKAT[2]

Keywords: Five-phase induction machine; Five-phase three-level inverter; Direct torque control, Dc-link voltages balancing strategy.

This paper proposes a direct torque control with dc voltages balancing strategy for a five-phase induction machine fed by a five-phase three-level diode-clamped inverter. The goal of the proposed multilevel direct toque control is not only to control the machine flux and torque but also to maintain the dc-bus voltage at the required level. This objective can be achieved by using a three-level direct torque control endowed with a balancing strategy based on the effective use of redundant switching states of the inverter voltage vectors. To make this clear, a set of simulation results is presented and discussed to verify the feasibility and effectiveness of the proposed control scheme.

1. INTRODUCTION

Multiphase machines have become serious contenders for safety-critical applications that require wide fault-tolerant capabilities and high system reliability such as electric ships, hybrid vehicles, and electric aircraft [1]. With the higher number of phases, and consequently the available degrees of freedom offered by multiphase machines, the motor power is split across the phases, thus, reducing the per-phase converter ratings, which is a highly desirable feature in medium-voltage applications [2].

Multiphase machines possess several advantages over conventional three phases such as: reducing the amplitude and increasing the frequency of torque pulsations, reducing the rotor harmonic currents and the current per phase without increasing the voltage per phase, lowering the dc-link current harmonics, and higher reliability [3].

Applications involving high power may require multiphase systems, to reduce stress on the switching devices. There are two approaches to supplying high-power electric drives; one approach is the use of multilevel inverters supplying three-phase machines and the other approach is the use of multi-leg inverters supplying multiphase machines. Combining these two aspects can offer much more features for the resulting multilevel multiphase drive [4].

Indeed, the multilevel inverters are suitable for electric drives since they do not lower only the output harmonics but also, they reduced the electromagnetic interference and common-mode voltage. The most common multilevel inverter topologies can be categorized mainly into the cascaded multilevel inverter, flying capacitor multilevel inverter and diode clamped multilevel inverter (DCI). The last-mentioned type represents one of the most interesting solutions, to increase voltage and power levels and achieve high-quality voltage waveforms [5]. This makes the DCI an attractive solution to high-power drive systems.

However, to take full benefits of the DCI-based multiphase drives, the problem of dc-link voltage balancing should be faced [6]. Over time, several methods have been proposed to suppress the unbalance of dc-link capacitors voltages. Some of these methods are based on adding a zero sequence or a dc offset to output voltage [7]. Other alternative methods add auxiliary power electronics circuitries to redistribute charges between capacitors [8]. Other interesting approaches are based on using switching vector redundancies to face the dc voltages fluctuation phenomenon [9].

Direct torque control (DTC), as opposed to the conventional flux-oriented control method, regulates the stator flux and electromagnetic torque of the electrical machine directly and independently [10]. So, the DTC can deliver excellent dynamic performance, which makes it indispensable in a plethora of industrial applications [3]. However, the DTC produces large torque and flux ripples. This unwanted feature can be attributed to the fact that the DTC applies a single voltage vector for the complete control cycle. In the classical DTC scheme using the two-level inverter, the torque and flux ripples are high due to the limited number of voltage vectors. To overcome this problem, many contributions have been made that extent DTC to multilevel topologies [11].

In this paper, the multilevel DTC with dc-link voltages balancing ability is proposed for a five-phase induction machine (FPIM) fed by a three-level diode clamped inverter. Two objectives are expected to be accomplished: balancing the voltages of the dc-link capacitors and ensuring high performance of the proposed multiphase drive.

The present paper structure is as follows. The model of the FPIM is presented in section 2. In section 3, the model of the three-level five-phase DCI is presented. To get the decoupling between the flux and torque, the three-level DTC approach is presented in section 4. The simulation results of the three-level DTC without a balancing strategy for FPIM are presented in section 5. Section 6 is reserved for balancing analysis and applied to the proposed control strategy. In section 7, finally, the simulation results related to the three-level DTC with balancing strategy are presented and discussed.

2. FIVE-PHASE INDUCTION MACHINE MODELING

The modeling of the FPIM is based on the usual assumptions such as the effect of saturation is neglected, and the distribution of induction along the air gap is sinusoidal [12]. The stator voltage equations of the FPIM are given by:

$$\begin{bmatrix} v_{sa} \\ v_{sb} \\ v_{sc} \\ v_{sd} \\ v_{se} \end{bmatrix} = \begin{bmatrix} R_s & 0 & 0 & 0 & 0 \\ 0 & R_s & 0 & 0 & 0 \\ 0 & 0 & R_s & 0 & 0 \\ 0 & 0 & 0 & R_s & 0 \\ 0 & 0 & 0 & 0 & R_s \end{bmatrix} \begin{bmatrix} i_{sa} \\ i_{sb} \\ i_{sc} \\ i_{sd} \\ i_{se} \end{bmatrix} + \frac{\mathrm{d}}{\mathrm{d}t} \begin{bmatrix} \phi_{sa} \\ \phi_{sb} \\ \phi_{sc} \\ \phi_{sd} \\ \phi_{se} \end{bmatrix}. \quad (1)$$

[1] Department of Electrical Engineering, University of Kasdi Merbah, Ouargla 30000, BP. 511, Algeria, lakhdarbenyoussef@yahoo.com
[2] Electrical Engineering Laboratory, Faculty of Technology, University of M'sila, M'sila 28000, BP. 166, Algeria, sa_barkati@yahoo.fr

The rotor voltage equations of the FPIM are given by:

$$\begin{bmatrix}0\\0\\0\\0\\0\end{bmatrix}=\begin{bmatrix}R_r&0&0&0&0\\0&R_r&0&0&0\\0&0&R_r&0&0\\0&0&0&R_r&0\\0&0&0&0&R_r\end{bmatrix}\begin{bmatrix}i_{ra}\\i_{rb}\\i_{rc}\\i_{rd}\\i_{re}\end{bmatrix}+\frac{\mathrm{d}}{\mathrm{d}t}\begin{bmatrix}\phi_{ra}\\\phi_{rb}\\\phi_{rc}\\\phi_{rd}\\\phi_{re}\end{bmatrix}, \quad (2)$$

with:

$[v_s]=[v_{sa}\quad v_{sb}\quad v_{sc}\quad v_{sd}\quad v_{se}]^T$: stator voltage vector;

$[i_s]=[i_{sa}\quad i_{sb}\quad i_{sc}\quad i_{sd}\quad i_{se}]^T$: stator current vector;

$[i_r]=[i_{ra}\quad i_{rb}\quad i_{rc}\quad i_{rd}\quad i_{re}]^T$: rotor current vector;

$[\phi_s]=[\phi_{sa}\quad \phi_{sb}\quad \phi_{sc}\quad \phi_{sd}\quad \phi_{se}]^T$: stator flux vector;

$[\phi_r]=[\phi_{ra}\quad \phi_{rb}\quad \phi_{rc}\quad \phi_{rd}\quad \phi_{re}]^T$: rotor flux vector.

Using the following transformation, the original five-phase system can be transformed into the stationary reference frame:

$$\left[X_\alpha \quad X_\beta\right]^T=[T]\left[X_a \quad X_b \quad X_c \quad X_d \quad X_e\right]^T. \quad (3)$$

In this transformation, the variable X can be used to stand for stator and rotor current vectors, stator and rotor flux vectors, or stator and rotor voltage vectors.

The matrix T is given by:

$$[T]=\sqrt{\frac{2}{5}}\times \times\begin{bmatrix}\cos(0)&\cos(2\pi/5)&\cos(4\pi/5)&\cos(6\pi/5)&\cos(8\pi/5)\\\sin(0)&\sin(2\pi/5)&\sin(4\pi/5)&\sin(6\pi/5)&\sin(8\pi/5)\end{bmatrix} \quad (4)$$

Using this transformation, the stator voltage $v_{s\alpha}$ and $v_{s\beta}$ equations can be written as:

$$\begin{bmatrix}v_{s\alpha}\\v_{s\beta}\end{bmatrix}=\begin{bmatrix}R_s&0\\0&R_s\end{bmatrix}\begin{bmatrix}i_{s\alpha}\\i_{s\beta}\end{bmatrix}+\frac{\mathrm{d}}{\mathrm{d}t}\begin{bmatrix}\phi_{s\alpha}\\\phi_{s\beta}\end{bmatrix}. \quad (5)$$

The rotor voltage $v_{r\alpha}$ and $v_{r\beta}$ equations can be written as:

$$\begin{bmatrix}v_{r\alpha}\\v_{r\beta}\end{bmatrix}=\begin{bmatrix}R_r&0\\0&R_r\end{bmatrix}\begin{bmatrix}i_{r\alpha}\\i_{r\beta}\end{bmatrix}+\frac{\mathrm{d}}{\mathrm{d}t}\begin{bmatrix}\phi_{r\alpha}\\\phi_{r\beta}\end{bmatrix}+ + p\Omega\begin{bmatrix}-1&0\\0&1\end{bmatrix}\begin{bmatrix}\phi_{r\alpha}\\\phi_{r\beta}\end{bmatrix} \quad (6)$$

with

$\left[v_{s\alpha\beta}\right]=\left[v_{s\alpha}, v_{s\beta}\right]^T$: α-β axis stator voltage vector;

$\left[i_{s\alpha\beta}\right]=\left[i_{s\alpha}, i_{s\beta}\right]^T$: α-β axis stator current vector;

$\left[\phi_{s\alpha\beta}\right]=\left[\phi_{s\alpha}, \phi_{s\beta}\right]^T$: α-β axis stator flux vector.

The torque can be calculated by:

$$T_e=p\left(\phi_{s\alpha}i_{s\beta}-\phi_{s\beta}i_{s\alpha}\right). \quad (7)$$

Mechanic equation is given by:

$$J\frac{\mathrm{d}\Omega}{\mathrm{d}t}=T_e-T_L-f\Omega, \quad (8)$$

with

T_e, T_L : electromagnetic and load torques;

J, f : inertia moment and friction coefficient;

Ω, p : rotor speed and pole pair number.

3. THREE-LEVEL FIVE-PHASE DCI MODELING

The schematic of the three-level five-phase inverter feeding a five-phase induction motor is shown in Fig. 1. The three-level five-phase inverter has 243 voltage vectors among them 240 are active and 3 are zero [5]. The switching function of these voltage vectors is represented as S_{xj} (with j = 1, 2, 3 or 4 and x=a, b, c, d or e), and S_{xi} = 2 or 0 or 1. Indeed, state 2 represents turning "*ON*" of the two upper switches, state 0 represents turning "*ON*" of the two lower switches, and state 1 represents turning "*ON*" of the two middle switches, whereas the other switches for each chosen state remain "*OFF*" [13].

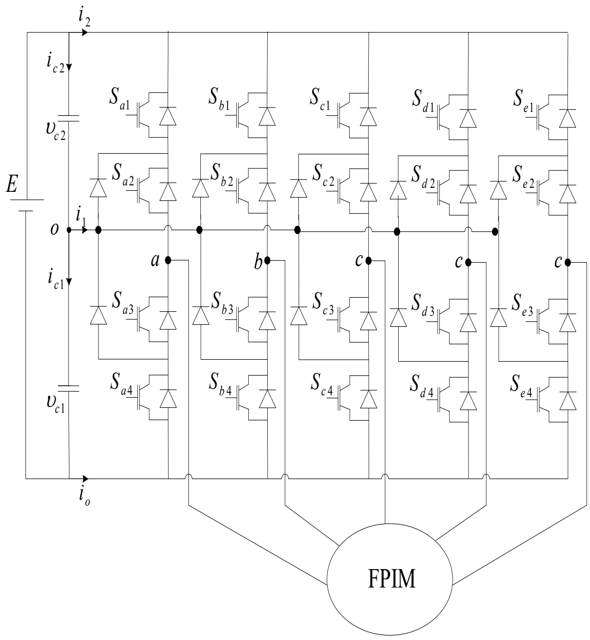

Fig. 1 – Schematic representation of a three-level five-phase DCI.

The switching functions can be expressed as:

$$\begin{cases}F_{x2}=S_{x1}S_{x2},\\F_{x1}=S_{x2}S_{x3}.\end{cases} \quad (9)$$

The instantaneous inverter phase to neutral voltages v_{sa}, v_{sb}, v_{sc}, v_{sd} and v_{se} can be expressed in terms of switching functions and dc-link capacitors voltages as follows:

$$\begin{bmatrix}v_{sa}\\v_{sb}\\v_{sc}\\v_{sd}\\v_{se}\end{bmatrix}=\begin{bmatrix}4F_{a2}-F_{b2}-F_{c2}-F_{d2}-F_{e2}&4F_{a1}-F_{b1}-F_{c1}-F_{d1}-F_{e1}\\4F_{b2}-F_{c2}-F_{d2}-F_{e2}-F_{a2}&4F_{b1}-F_{c1}-F_{d1}-F_{e1}-F_{a1}\\4F_{c2}-F_{d2}-F_{e2}-F_{a2}-F_{b2}&4F_{c1}-F_{d1}-F_{e1}-F_{a1}-F_{b1}\\4F_{d2}-F_{e2}-F_{a2}-F_{b2}-F_{c2}&4F_{d1}-F_{e1}-F_{a1}-F_{b1}-F_{c1}\\4F_{e2}-F_{a2}-F_{b2}-F_{c2}-F_{d2}&4F_{e1}-F_{a1}-F_{b1}-F_{c1}-F_{d1}\end{bmatrix}\times \times\begin{bmatrix}\upsilon_{c1}+\upsilon_{c2}\\\upsilon_{c1}\end{bmatrix} \quad (10)$$

4. THREE-LEVEL FIVE-PHASE DTC PRINCIPLE

The basic idea of conventional DTC is to perform the closed-loop control of stator flux and electromagnetic torque by selecting the appropriate stator voltage vectors from a switching table as a function of the stator flux and the electromagnetic torque deviations given by two hysteresis comparators [3].

The α-β components of stator voltage are estimated by:

$$\left[\hat{v}_{s\alpha\beta}\right]^T = [T]\left[\hat{v}_s\right], \tag{11}$$

with $\hat{v}_s = \left[\hat{v}_{sa} \quad \hat{v}_{sb} \quad \hat{v}_{sc} \quad \hat{v}_{sd} \quad \hat{v}_{se}\right]^T$ is estimated using (10).

The α-β components of stator flux are estimated by:

$$\hat{\phi}_{s\alpha\beta} = \int_0^t \left(\hat{v}_{s\alpha\beta} - R_s i_{s\alpha\beta}\right) \mathrm{d}\,\tau + \hat{\phi}_{s\alpha\beta}(0). \tag{12}$$

The magnitude and angle of stator flux are estimated by:

$$\begin{cases} \left|\hat{\phi}_s\right| = \sqrt{\hat{\phi}_{s\alpha}^2 + \hat{\phi}_{s\beta}^2}, \\ \hat{\theta}_s = \tan 2^{-1}\left(\hat{\phi}_{s\beta} / \hat{\phi}_{s\alpha}\right) \end{cases} \tag{13}$$

The torque can be estimated by:

$$\hat{T}_e = p\left(\hat{\phi}_{s\alpha} i_{s\beta} - \hat{\phi}_{s\beta} i_{s\alpha}\right). \tag{14}$$

Figure 2 shows the space vector representation of the voltage vectors for the three-level five-phase DCI. In this space vector diagram, the vectors are divided into five groups according to their amplitudes [5]: first group $(v_1 \to v_{10})$, second group $(v_{11} \to v_{20})$, third group $(v_{21} \to v_{30})$, fourth group $(v_{31} \to v_{40})$, and fifth group $(v_{41} \to v_{50})$.

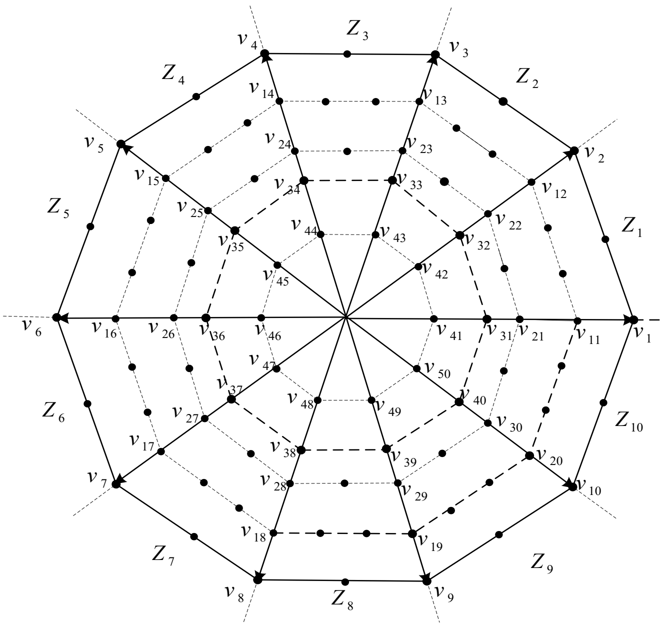

Fig. 2 – Space vector diagram for the three-level five-phase DCI.

Table 1 shows the selection of the switching vector for the DTC of FPIM fed by a five-phase three-level DCI.

Table 1

Switching states table adopted for the three-level DTC.

Φ	τ	Z_i	Φ	τ	Z_i
1	4	$v_{(i+1)}$	-1	4	$v_{(i+4)}$
	3	$v_{(i+11)}$		3	$v_{(i+14)}$
	2	$v_{(i+21)}$		2	$v_{(i+24)}$
	1	$v_{(i+31)}$		1	$v_{(i+34)}$
	0	$v_{(i+40)}$		0	$v_{(i+45)}$
	-1	$v_{(i+39)}$		-1	$v_{(i+36)}$
	-2	$v_{(i+29)}$		-2	$v_{(i+26)}$
	-3	$v_{(i+19)}$		-3	$v_{(i+16)}$
	-4	$v_{(i+9)}$		-4	$v_{(i+6)}$

The scheme of direct torque control of the FPIM fed by a three-level DCI is presented in Fig. 3.

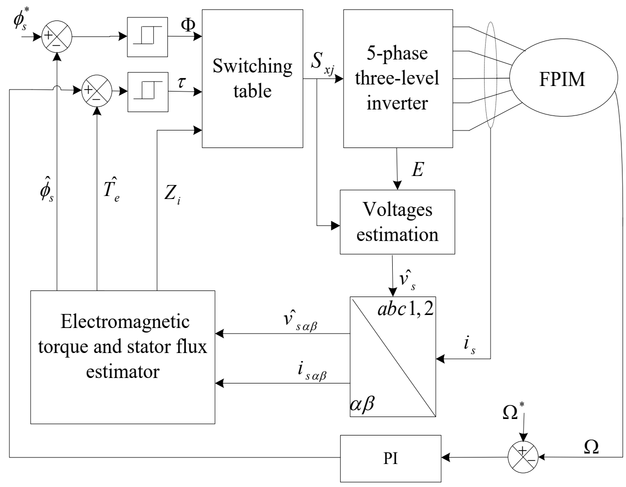

Fig. 3 – Schematic diagram of three-level DTC for FPIM (j =1, 2, 3, 4, or 5).

5. SIMULATION RESULTS OF DTC WITHOUT BALANCING STRATEGY

To verify the validity of the three-level DTC approach, the drive system was simulated using the FPIM parameters given in Appendix. The dc side of the three-level DCI is supplied by a constant dc source of 600 V. The simulation results are obtained using the following dc-link capacitors values $C_1 = C_2 = 1$ mF.

To test the performance of the system drive, the five-phase induction machine is started from a standstill with a reference speed of 100 rad/s, and it is loaded by 8 N.m. At time t =1 s, the load torque is changed from 8 Nm to 0 Nm followed by a speed inversion from 100 rad/s to -100 rad/s at t =1.5 s. Fig. 4 presents the simulation results obtained with DTC without balancing strategy for dc-link voltages.

The simulation results show that the rotor speed and the stator flux response follow exactly their reference one and the decoupling between the electromagnetic torque and stator flux is maintained during the speed and torque load variations.

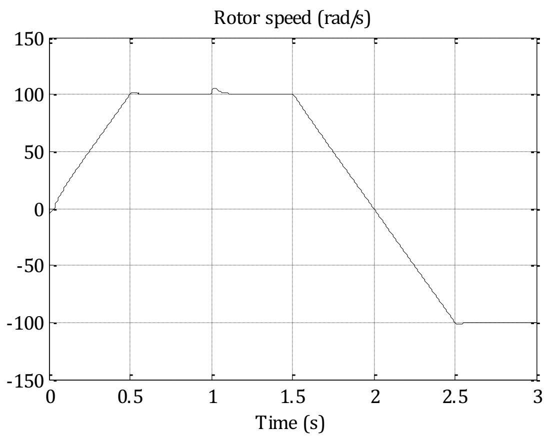

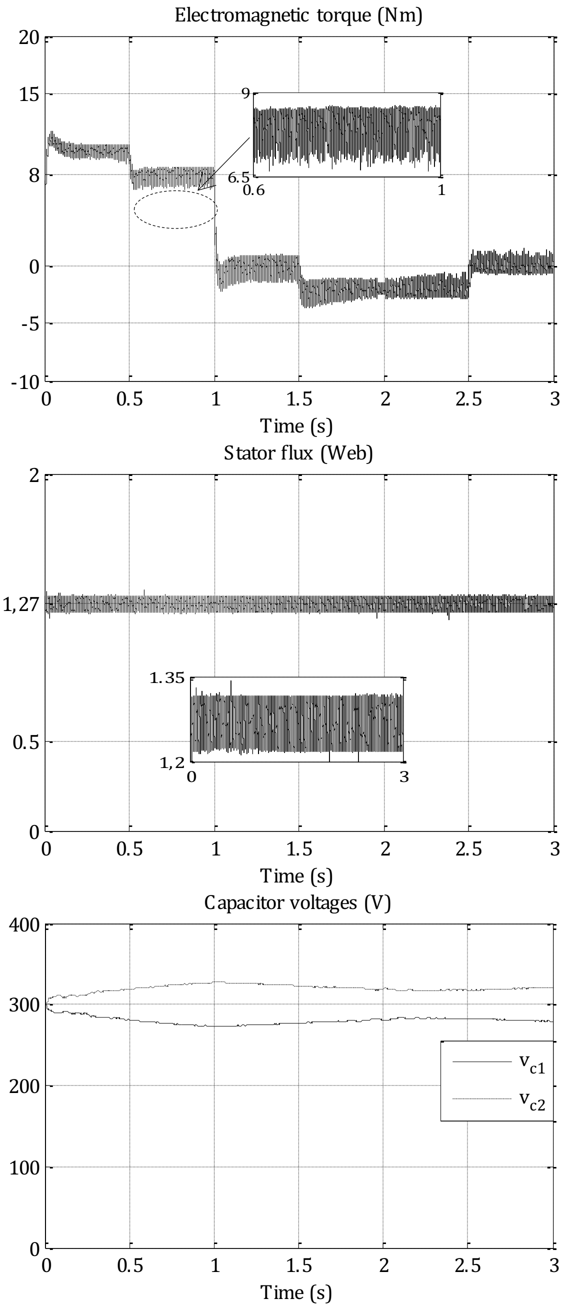

Fig. 4 – Simulation results of three-level DTC of FPIM without balancing strategy.

However, it can be seen perfectly the problem of the unbalance of the two dc voltages of the intermediate capacitors filter. Indeed, the voltages v_{c1} decrease, and the voltages v_{c2} increase. To improve the performance of the three-level DTC of FPIM, the three-level DTC based on a balancing mechanism is proposed.

6. CAPACITOR VOLTAGE BALANCING STRATEGY

The balancing method proposed in this paper is based on the minimum energy property fulfilled by selecting appropriate redundant switching states of the inverter over a switching period [14].

In a three-level five-phase DCI, the total energy W of the two capacitors is:

$$W = \frac{1}{2}\sum_{q=1}^{2} C_q \upsilon_{cq}^2 . \quad (15)$$

If all capacitors have equal capacitance, $C_1 = C_2 = C$, a control method should minimize the cost function F and consequently achieve voltage balancing [6]. By a change of variable from υ_{cq} to $(\upsilon_{cq} - E/2)$ in (15), a positive definite cost function F is defined which reaches zero as the absolute minimum value: $F = \frac{1}{2} C \sum_{q=1}^{2} \Delta\upsilon_{cq}^2$,(16)

with: $\Delta\upsilon_{cq} = \upsilon_{cq} - E/2$. The capacitor voltages are maintained at voltage reference values of $(E/2)$.

The condition to minimize the previous defined cost function is:

$$\frac{\mathrm{d}F}{\mathrm{d}t} = C\sum_{q=1}^{2} \Delta\upsilon_{cq} \frac{\mathrm{d}\upsilon_{cq}}{\mathrm{d}t} = \sum_{q=1}^{2} \Delta\upsilon_{cq} i_{cq} \le 0 , \quad (17)$$

with: i_{cq}: current of the capacitor C_q. From Fig. 1, the capacitor currents are expressed as:

$$i_{c2} = i_1 + i_{c1} . \quad (18)$$

By substituting i_{c2} calculated from (18) into (17), the following condition to achieve voltage balancing is deduced:

$$\frac{1}{2}\sum_{q=1}^{2} \Delta\upsilon_{cq} i_1 \le 0 . \quad (19)$$

Considering a constant dc-link voltage:

$$\sum_{q=1}^{2} \Delta\upsilon_{cq} = 0 , \quad (20)$$

and substituting $\Delta\upsilon_{c2}$ calculated from (20) in (19), it yields:

$$\Delta\upsilon_{c1} i_1 \ge 0 . \quad (21)$$

Applying the averaging operator, over one sampling period to (21) results:

$$\frac{1}{T}\int_{PT}^{(P+1)T} \left(\Delta\upsilon_{c1} i_1\right)\mathrm{d}t \ge 0 . \quad (22)$$

Equation (22) is simplified to:

$$\Delta\upsilon_{c1}(P)\bar{i}_1(P) \ge 0 . \quad (23)$$

with: $\Delta\upsilon_{c1}(P)$: Voltage drifts of C_1 at sampling period P, where $\bar{i}_1(P)$ is the averaged value of the first dc-side intermediate branch current.

Using (23), the function F is given by:

$$F = \Delta\upsilon_{c1}(P)\bar{i}_1(P) . \quad (24)$$

The relationship between the dc i_1 and ac side currents, i_{sa}, i_{sb}, i_{sc}, i_{sd}, and i_{se}, is given by:

$$i_1 = F_{a1} i_{sa} + F_{b1} i_{sb} + F_{c1} i_{sc} + F_{d1} i_{sd} + F_{e1} i_{se} . \quad (25)$$

The current $\bar{i}_1$ is calculated based on (25) for each set of switching combinations, and it is replaced in (24). Then, the best set that minimizes (24) is selected.

Table 2 presents an example for the switching states of the vectors v_{32}, v_{42}.

Table 2

Switching states of the vectors v_{32}, v_{42}.

Vectors	v_{32}			v_{42}	
States	11000	22111		11101	22212
i_1	$i_{sa}+i_{sb}$	$i_{sc}+i_{sd}+i_{se}$		$-i_{sd}$	i_{sd}

The three-level DTC scheme including the dc capacitor voltage control strategy is shown in Fig. 5.

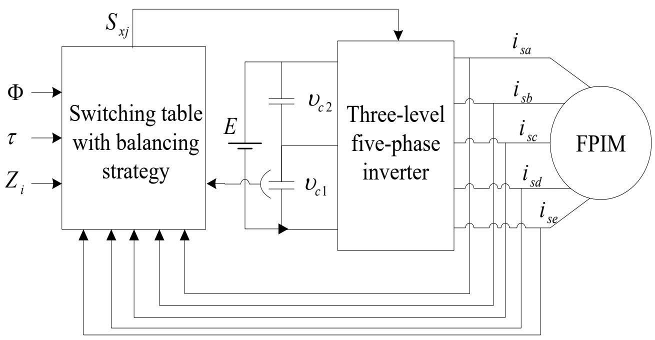

Fig. 5 – Schematic diagram of the three-level DTC of FPIM including a dc-link voltages balancing strategy.

7. **SIMULATION RESULTS OF DTC WITH BALANCING STRATEGY**

The obtained results of three-level DTC with balancing strategy, using the same simulation conditions used in Fig. 4, are illustrated in Fig. 6.

As it can be seen from Fig. 6, the use of a three-level DTC equipped with a balancing strategy permit obtaining the same dynamic performances as those obtained without a balancing strategy. Note also that the obtained results show that the DTC with balancing strategy control decrease the electromagnetic torque and stator flux ripples in comparison with those obtained by that without balancing strategy.

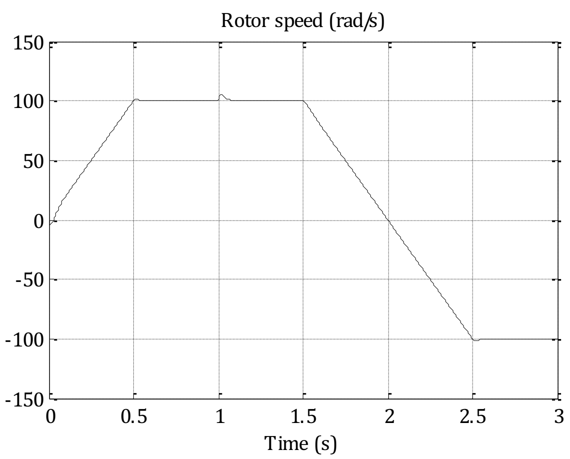

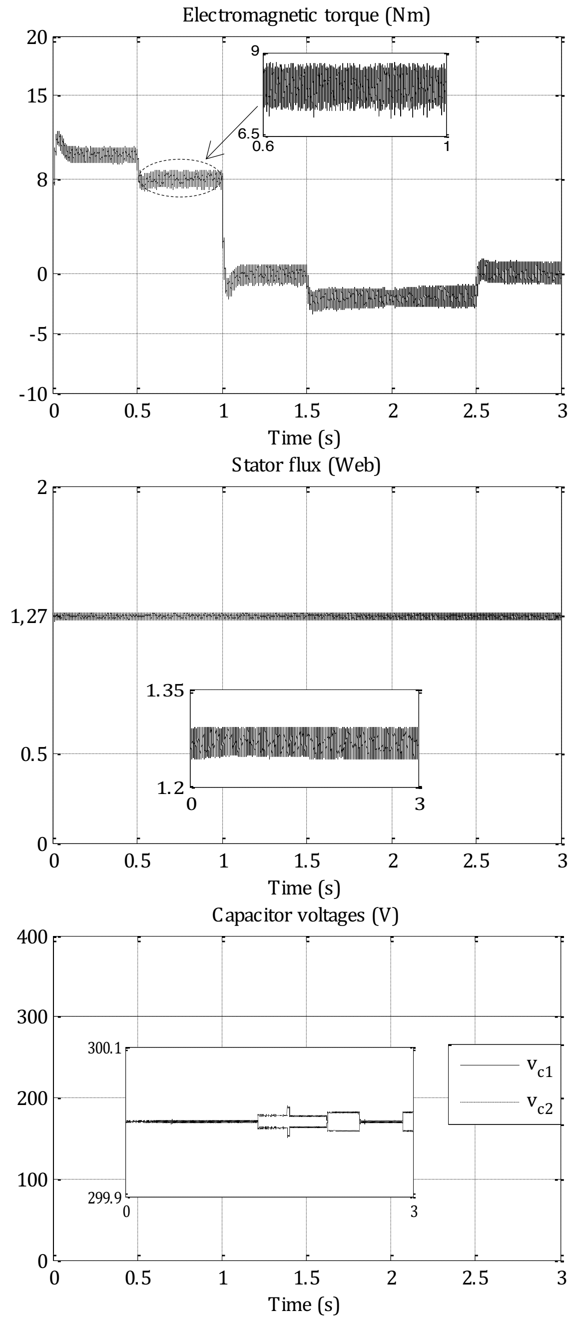

Fig. 6 – Simulation results of three-level DTC of FPIM with balancing strategy.

It is important to note that the application of the proposed redundant vectors based on three-level DTC control of the five-phase IM maintains the capacitor voltages v_{c1} and v_{c2} constant around their reference value of 300 V.

8. **CONCLUSION**

In this paper, a direct torque control associated with a dc voltage balancing strategy is adopted to control a five-phase machine fed by a three-level five-leg DCI. The simulation results confirm that this approach allows a total decoupling between the flux and torque at any operating point. Therefore, this control strategy can give a higher performance in transient phases such as the step change of the speed reference and the torque load. The simulation results show also that the objective of maintaining balanced capacitors voltages in dc-link is carried out effectively with the adopted three-level DTC equipped with a balancing strategy.

APPENDIX

The parameters of the five-phase induction machine are given as follows:

R_s=10 Ω, R_r=6 Ω, L_s=0.46 H, L_r=0.46 H, M=0.42 H, J=0.01 Nms^2/rad, ϕ_{sn} = 1.2705 Wb, T_{Ln}=8.33 Nm.

Received on 24 January 2021.

REFERENCES

1. P. Zhong, Z. Zedong, L. Yongdong, L. Zicheng, *Sensorless vector control of multiphase induction machine based on full-order observer and harmonic suppression*, IEEE, 3rd International Future Energy Electronics Conference, and ECCE Asia, pp. 2153–2160 (2017).
2. M. Cristina, R. Manuel, B. Federico, J. Mario, G. Ignacio, *variable sampling time model predictive control of multiphase induction machines*, IEEE, 15th International Workshop on Advanced Motion Control, pp. 287-292 (2018).
3. X. Wang, W. Zheng, X. Zhixian, *A hybrid direct torque control scheme for dual three-phase PMSM drives with improved operation performance*, IEEE Transactions on Power Electronics, **34**, *2*, pp. 1622-1634 (2019).
4. C. Neugebauer, J. Perreault, H. Lang, C. Livermore, *A six-phase multilevel inverter for MEMS electrostatic induction micro motors*, IEEE Transactions on Circuits and Systems, **51**, *2*, pp. 49-56 (2004).
5. D. Obrad, M. Jones, L. Emil, *A comparison of carrier-based and space vector PWM techniques for three-level five-phase voltage source inverters*, IEEE Transactions on Industrial Informatics, **9**, *2*, pp. 609-619, (2013).
6. Z. Huibin, J. Stephen, A. Massoud, B. Williams, *An SVM algorithm to balance the capacitor voltages of the three-level NPC active power filter*, IEEE Transactions on Power Electronics, **23,** *6*, pp. 2694-2702 (2008).
7. H. Kalpesh, P. Agarwal, *Space vector modulation with dc-link voltage balancing control for three-level inverters*, International Journal of Recent Trends in Engineering, **1**, *3*, pp. 229-233 (2009).
8. R. Chibani, E. Berkouk, *Five-level PWM current rectifier – five-level NPC VSI permanent magnet synchronous machine cascade*, European Physical Journal-Applied Physics, **30**, pp. 135-148 (2005).
9. Y. Liu, J. Arrillaga, N. Watson, *Capacitor voltage balancing in multi-level voltage reinjection (MLVR) converters*, IEEE Transactions on Power Delivery, **20**, *2*, pp. 1728-1737 (2005).
10. C. Young, H. Choi, J. Jung, *Feedback linearization direct torque control with reduced torque and flux ripples for IPMSM drives*, IEEE Transactions on Power Electronics, **31**, *5*, pp. 3728-3737 (2016).
11. W. Yuhua, M. Jianlin, *Fuzzy based direct torque control for three-level inverter traction motor*, International Conference on Computer, Mechatronics, Control, and Electronic Engineering, pp. 191-194, (2010).
12. L. Alberto, C. Scharlau, A. Fernando, S. Haffner, *Influence of saturation on the air gap induction waveform of five-phase induction machines*, IEEE Transactions on Energy Conversion, **27**, *1*, pp. 29-41 (2012).
13. G. Liliang, E. Fletcher, *A space vector switching strategy for three-level five-phase inverter drives*," IEEE Transactions on Industrial Electronics, **57**, *7*, pp. 2332-2343 (2010).
14. Zhang, N. Wang, J. Hong, T. Yin, Z. Ziwei, S. Zeliang, *An optimal control algorithm of capacitor voltage balancing for modular multilevel converter*, IEEE, Applied Power Electronics Conference and Exposition, pp. 3504-3507 (2019).